

(OCS)₃ van der Waals Complex: A Theoretical Study

H. Valdés and J. A. Sordo*

Laboratorio de Química Computacional, Departamento de Química Física y Analítica, Facultad de Química, Universidad de Oviedo, Julián Clavería 8, 33006 Oviedo, Principado de Asturias, Spain

Received: June 26, 2003; In Final Form: July 22, 2003

Ab initio calculations [MP2, MP4SDTQ, and QCISD(T)] using different basis sets [6-31G(d,p), cc-pVXZ (X = D, T, Q), and aug-cc-pVDZ] were carried out to explore the potential energy surface of (OCS)₃. Six minimum energy structures were located and characterized. The most stable one corresponds to an antiparallel arrangement of the monomers, in agreement with microwave spectroscopic experiments. The nature of the interactions present in the trimer was analyzed by using the Symmetry Adapted Perturbation Theory. The importance of the induction forces in this type of system suggests that results from semiempirical potentials with no inclusion of this component should be considered with extreme caution. The analysis helps to rationalize the experimentally observed preference for the antiparallel arrangement. Two transition structures corresponding to the interconversion of enantiomeric forms of the parallel and the most stable of the antiparallel arrangements were located on the potential energy surface. The relatively high energy barrier between them is consistent with the very small splittings exhibited by the rotational lines of the microwave spectra.

Introduction

The use of advanced experimental techniques,¹ especially molecular beam Fourier transform microwave spectroscopy,^{2,3} has made the systematic study of trimer structures accessible during the past decade. Such studies represent a preliminary step toward the rationalization of the mechanism of formation of cluster structures, and in the limit, to a better understanding of the condensed phase of matter.

In 1996, Connelly et al., while looking for the OCS dimer using a pulsed nozzle Fourier transform spectrometer, discovered the OCS trimer.⁴ Their data from a single isotopomer did not permit a unique structure determination, and two possible isomers consistent with the observed rotational constants were identified, namely, one antiparallel trimer and one parallel arrangement. These authors employed a semiempirical potential,⁵ based on the combination of electrostatic interactions between distributed multipoles on different monomers and atom–atom Lennard potential to describe the dispersion and repulsion interactions, to explore the potential energy surface (PES) of the OCS dimer and trimer. This simple model helped them to conclude that the trimer observed is present as an antiparallel asymmetric arrangement (where one sulfur atom is pointing in an opposite direction to the other two sulfur atoms in the trimer), 100 cm⁻¹ lower in energy than the parallel trimer (where the three sulfur atoms in the trimer are pointing in the same direction). Using the same potential model, Connelly et al. estimated the tunneling barriers associated with stereo-isomerization (100 cm⁻¹ for the antiparallel transition structure and 117 cm⁻¹ for the parallel arrangement), which allowed them to explain the splitting observed in the a- and c-type transitions.

More recently, Peebles and Kuczkowski⁶ extended Connelly's original work by assigning two additional isotopomers and determined the dipole moment components of the OCS trimer. They concluded that the antiparallel conformer is the one observed. The use of the semiempirical ORIENT model⁷ led

them to locate four minima structures (three barrel-like and one planar cyclic). Using an appropriate set of empirical parameters, the ORIENT predicted geometry, slightly different from that computed by Connelly et al., was in very good agreement with the experimental structure. However, Peebles and Kuczkowski concluded that some of the parameters in the ORIENT model that were appropriate for predicting accurate dimer structures were not necessarily appropriate for trimers. Indeed, it has been reported that using the ORIENT default parameters has given poor agreement between experimental and theoretical predictions for a number of systems.⁸ This represents the eternal dilemma associated with the use of semiempirical methods with adjustable parameters. A further drawback in the use of the above-mentioned semiempirical potentials is the lack of an appropriate term to represent the induction forces whose contributions can be relevant in a number of cases. It should be expected that in such cases further ab initio studies would be a significant step toward a much better understanding of the structures of van der Waals (vdW) systems.⁹

The analysis of the changes in structural parameters when comparing the OCS dimer structure to the dimer faces of the trimer, particularly the loss of planarity in all faces of the trimer, was qualitatively related to the fact that the balance between electrostatic, dispersion, and repulsion forces in the trimers is different from that in the corresponding dimers.⁶

In recent contributions from this laboratory,^{10–12} it has been shown that ab initio methodology can be used as an appropriate tool to complement experimental studies on trimers. Particularly, the use of the Symmetry Adapted Perturbation Theory (SAPT)¹³ has proved useful to analyze, in a quantitative way, the balance between the physically meaningful forces acting in the clusters, namely, electrostatic, induction, dispersion, and exchange. On the other hand, in the present case we will study the dynamics corresponding to the interconversion between equivalent structures giving rise to the observed splittings in the rotational spectra. The location of the appropriate transition structures on the ab initio PES as well as the estimation of their associated

* Corresponding author. Fax: +34 985237850. E-mail: jasg@correo.uniovi.es.

energy barriers has been shown to be the appropriate tools to be used in this regard.^{14–16}

Theoretical Methods

The PES of the (OCS)₃ vdW system has been extensively explored using ab initio methodology. MP2 optimizations using both Pople's 6-31G(d,p)¹⁷ and Dunning's^{18,19} cc-pVDZ, aug-cc-pVDZ, and cc-pVTZ basis sets were carried out. All the structures located on the PES were characterized as minima or transition structures by computing and diagonalizing the Hessian matrix. On the other hand, bonding interactions in the trimer structures were also characterized by means of Bader's topological analysis of the corresponding charge density.²⁰

To obtain reliable energies, further MP4SDTQ and QCISD(T) (including contributions from the very important triple excitations) single-point calculations were performed. The basis set superposition error (BSSE) was estimated by following two different strategies: the classical counterpoise procedure (CP)²¹ and by estimating the complete basis set (CBS) limit from a series of cc-pVDZ, cc-pVTZ, and cc-pVQZ calculations at the MP2 level.²² All the supermolecular calculations were carried out with the GAUSSIAN 98 packages of programs, using standard integral cutoffs and convergence criteria.²³

The theoretical scheme just described has been systematically employed in a number of studies (see refs 10–12 and references therein) providing valuable information that complemented the experimental data available.

SAPT methodology¹³ was applied to quantify the different contributions to the interaction energy. The SAPT expansion for the interaction energy we used can be written as

$$E_{\text{int}}(\text{SAPT}) = E_{\text{int}}^{\text{HF}} + E_{\text{int}}^{\text{CORR}} \quad (1)$$

where $E_{\text{int}}^{\text{HF}}$ represents low-order corrections contained in the supermolecule Hartree–Fock (HF) interaction energy

$$E_{\text{int}}^{\text{HF}} = E_{\text{pol}}^{(10)} + E_{\text{exch}}^{(10)} + E_{\text{ind,r}}^{(20)} + E_{\text{exch-ind,r}}^{(20)} + \delta E_{\text{int}}^{\text{HF}} \quad (2)$$

with $\delta E_{\text{int}}^{\text{HF}}$ collecting all higher-order induction and exchange corrections contained in $E_{\text{int}}^{\text{HF}}$ and not computed by the SAPT code (r indicates that the corresponding term was computed with the inclusion of the coupled HF response of the perturbed system).¹³

$E_{\text{int}}^{\text{CORR}}$ contains the correlated portion of the interaction energy approximated by SAPT as

$$E_{\text{int}}^{\text{CORR}} = E_{\text{pol,r}}^{(12)} + E_{\text{exch}}^{(11)} + E_{\text{exch}}^{(12)} + {}^tE_{\text{ind}}^{(22)} + {}^tE_{\text{exch-ind}}^{(22)} + E_{\text{disp}}^{(20)} + E_{\text{exch-disp}}^{(20)} \quad (3)$$

where the t superscript indicates that the true correlation effects,¹³ which represent those parts of the $E_X^{(22)}$ contributions that are not included in the terms $E_X^{(20)}$ in eq 3, are considered (see for further details in the notation of ref 13).

It can be shown²⁴ that the results obtained in eq 1 for $E_{\text{int}}^{\text{CORR}}$ (SAPT), using eqs 2 and 3, tend asymptotically to the values that would be calculated at the supermolecular MP2 level. SAPT calculations were carried out with the aug-cc-pVDZ basis set, which includes diffuse functions, as the role played by the dispersion contributions in the systems under study is expected to be relevant.

Results and Discussion

Geometries. Figure 1 shows the geometries for the six minima structures located on the PES of (OCS)₃ as computed

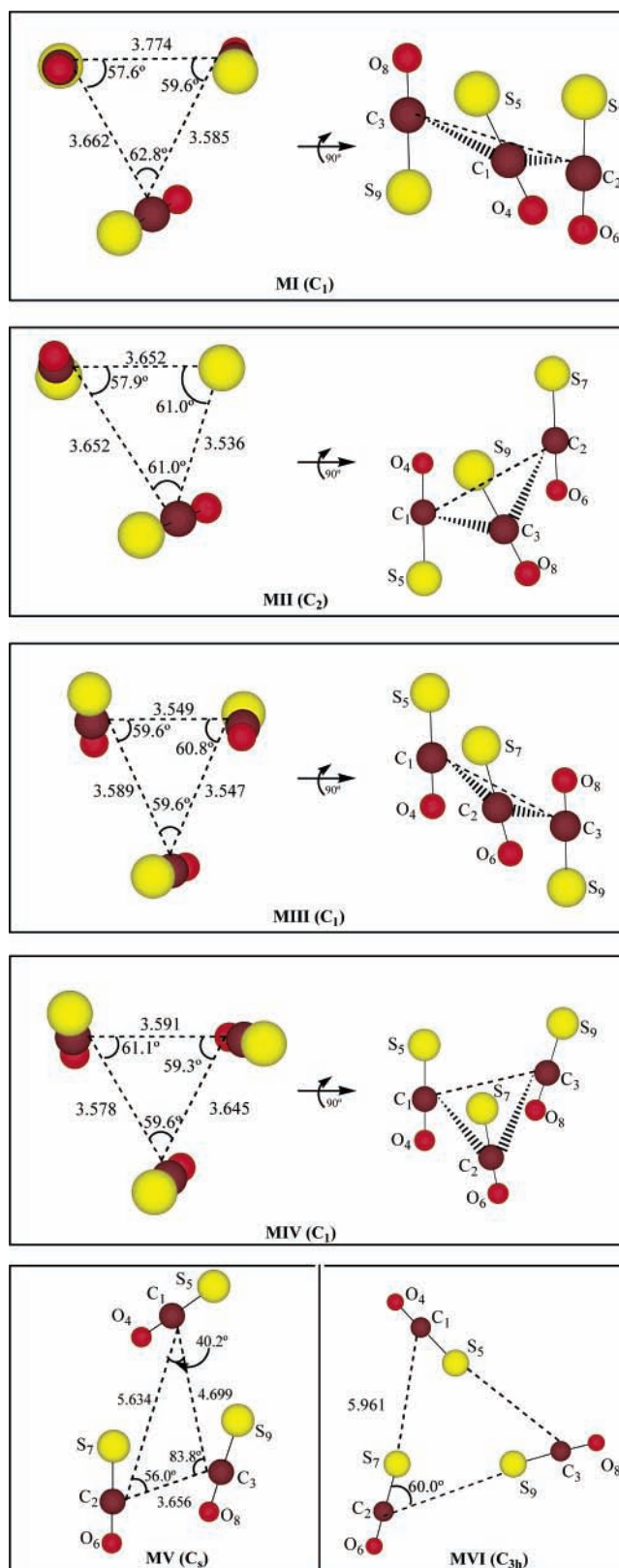


Figure 1. (OCS)₃ vdW complex structures MI–MVI as computed at the MP2/cc-pVTZ level of theory. Distances are given in angstroms and angles in degrees. Further structural parameters are given in Table 1 and as Supporting Information.

at the MP2/cc-pVTZ level of theory (geometries as computed with the rest of the basis sets employed in this work are available as Supporting Information). Three barrel-like antiparallel structures (MI–MIII), one barrel-like parallel structure (MIV), and two planar structures (MV–MVI) were located. Other C_s

TABLE 1: MP2/cc-pVTZ Most Representative Geometrical Parameters for the Minima Structures Localized on the Potential Energy Surface of (OCS)₃^a

parameters	exptl ^b	structure					
		MI	MII	MIII	MIV	MV	MVI
r(C ₁ -C ₂)	3.654	3.585	3.652	3.589	3.578	5.634	5.961
r(C ₁ -C ₃)	3.797	3.662	3.652	3.549	3.591	4.699	5.961
r(C ₂ -C ₃)	3.908	3.774	3.536	3.547	3.645	3.656	5.961
∠(C ₁ -C ₂ -C ₃)	60.2	59.6	61.0	59.6	59.6	56.0	60.0
∠(C ₂ -C ₃ -C ₁)	56.6	57.6	61.0	60.8	59.3	83.8	60.0
∠(C ₃ -C ₁ -C ₂)	63.2	62.8	57.9	59.6	61.1	40.2	60.0
∠(S ₅ -C ₁ -C ₃)	70.9	76.3	77.0	117.5	78.4	102.7	4.2
∠(S ₇ -C ₂ -C ₁)	82.8	78.5	121.8	78.4	79.2	18.1	4.2
∠(O ₈ -C ₃ -C ₂)	116.5	109.1	63.5	63.0	57.6	58.3	175.9
τ(S ₅ -C ₁ -C ₃ -C ₂)	136.4	133.4	80.1	109.8	133.3	180.0	0.0
τ(S ₇ -C ₂ -C ₁ -C ₃)	80.0	75.3	105.1	131.2	79.6	0.0	0.0
τ(O ₈ -C ₃ -C ₂ -C ₁)	89.9	94.6	125.3	72.6	-72.3	180.0	180.0
τ(S ₅ -C ₁ -C ₃ -S ₉)	-156.2	-150.6	-148.7	-142.8	21.1	0.0	0.0
τ(S ₇ -C ₂ -C ₁ -S ₅)	32.7	21.5	21.2	24.8	24.6	180.0	0.0
τ(S ₉ -C ₃ -C ₂ -S ₇)	-178.8	-172.6	-168.2	-163.2	21.9	0.0	0.0

^aDistances are given in angstroms and angles in degrees. ^b See ref 6.

TABLE 2: MP2/cc-pVTZ Rotational Constants (MHz) and Dipole Moments (Debye) for the Minima Structures Localized on the Potential Energy Surface of (OCS)₃

structure	A	B	C	μ
MI	869.7	757.9	609.7	0.582
MII	994.7	664.7	511.2	0.574
MIII	951.0	656.0	450.8	0.612
MIV	873.2	748.1	533.6	1.595
MV	1297.8	436.6	326.7	1.761
MVI	547.1	547.1	273.6	0.0
exptl ^a	847.97958(2)	736.17579(2)	574.32591(1)	0.653(8)

^a See refs 4 and 6.

structures similar to **MV** with different relative dispositions of the OCS units were characterized as first- or second-order saddle points. In the case of the transition structures, the imaginary frequency was too small (less than 10 cm⁻¹) to be significant. In any case, if these structures were minima, their computed stability resulted lower than that of the less stable structure **MVI**, and consequently, they were not included in Figure 1. Table 1 collects the most representative geometrical parameters and Table 2 the rotational constants and dipole moments, as computed at the MP2/cc-pVTZ level, for the minima structures in Figure 1 (the corresponding data for the rest of the basis sets employed are available as Supporting Information).

As in our previous works on similar systems,^{10,11} the geometries computed with the various basis sets do not differ too much from each other. Examination of the MP2/cc-pVTZ geometrical parameters, rotational constants, and dipole moments leads us to conclude that structure **MI** corresponds to the one experimentally reported.^{4,6} The degree of agreement between the experimental data and the theoretical predictions is reasonably good when considering that the theoretical values correspond to equilibrium structure (r_e), while the experimental ones are vibrationally averaged values (r_0). Indeed, discrepancies of even 0.05 Å and 5° between r_e and r_0 structures can be expected.⁶

The six minima located on the PES were topologically characterized as structures with six intramolecular bond critical points (corresponding to the covalent bonds), three intermolecular bond critical points (one for each dimer face), and one ring critical point, defining a (9,9,1,0) characteristic set²⁰ (this topological information is available as Supporting Information).

Energetics. Table 3 contains the dissociation energies for the minima structures located on the PES for (OCS)₃ as estimated at different levels of theory (the corresponding results

TABLE 3: Dissociation Energies^a (kcal mol⁻¹/cm⁻¹) Calculated with the aug-cc-pVDZ and the cc-pVTZ Basis Sets at Different Theoretical Levels for the Minima Structures Located on the Potential Energy Surface of (OCS)₃

structure	bases	method		
		MP2	MP4SDTQ ^b	QCISD(T) ^b
MI	aug-cc-pVDZ	6.6/2340	6.6/2320	5.1/1792
	cc-pVTZ	4.9/1714		
MII	aug-cc-pVDZ	6.1/2160	6.2/2194	5.0/1753
	cc-pVTZ	4.5/1576		
MIII	aug-cc-pVDZ	5.8/2020	6.0/2109	4.9/1733
	cc-pVTZ	4.2/1472		
MIV	aug-cc-pVDZ	6.2/2173	6.2/2190	4.9/1721
	cc-pVTZ	4.6/1605		
MV	aug-cc-pVDZ	5.0/1764	5.0/1752	4.1/1435
	cc-pVTZ	3.5/1242		
MVI	aug-cc-pVDZ	3.9/1362	3.6/1244	1.4/1028
	cc-pVTZ	2.4/831		

^a Zero-point energy correction estimated at the MP2/cc-pVDZ level.

^b MP4SDTQ//MP2 and QCISD(T)//MP2 single-point calculations.

TABLE 4: Complete Basis Set (CBS) Limit Dissociation Energies (kcal mol⁻¹/cm⁻¹) Computed with the Series MP2/cc-pVXZ (X = D, T, Q) for the Minima Structures Located on the Potential Energy Surface of (OCS)₃

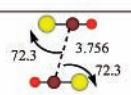
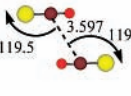
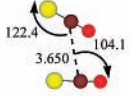
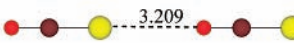
bases	MI	MII	MIII	MIV	MV	MVI
cc-pVDZ	3.8/1342	3.6/1259	3.5/1225	3.8/1353	3.2/1114	2.0/709
cc-pVTZ ^a	4.9/1714	4.5/1576	4.2/1472	4.6/1605	3.5/1242	2.4/831
cc-pVQZ ^{a,b}	5.4/1894	4.8/1701	4.4/1543	4.9/1723	3.9/1360	2.9/976
CBS/MP2	5.7/2002	5.0/1774	4.5/1583	5.1/1794	4.1/1434	3.1/1071

^a Zero-point energy correction estimated at the MP2/cc-pVDZ level.

^b MP2/cc-pVQZ//MP2/cc-pVTZ single-point calculations.

with 6-31G(d,p) and cc-pVDZ basis sets are also available as Supporting Information), and Table 4 collects the BSSE-free CBS extrapolations. **MI** is the most stable structure in all cases. The second structure in stability is the parallel arrangement **MIV**, 208 cm⁻¹ less stable than **MI** at the CBS/MP2 level. The two additional antiparallel structures are relatively close in energy to **MI** and **MIV**, and finally, the two planar structures **MV** and **MVI** are much less stable.

TABLE 5: Dissociation Energies (cm^{-1}) for the Different OCS·OCS Dimers Located on the Potential Energy Surface at Different Theoretical Levels^a

	MP2	MP4SDTQ ^c	QCISD(T) ^c
OCS·OCS (a)^b 			
aug-cc-pVDZ	887	880	716
cc-pVTZ	660		
OCS·OCS (b) 			
aug-cc-pVDZ	698	746	655
cc-pVTZ	534		
OCS·OCS (c) 			
aug-cc-pVDZ	788	793	657
cc-pVTZ	604		
OCS·OCS (d) 			
aug-cc-pVDZ	585	627	536
cc-pVTZ	404		

^a Some representative geometrical parameters (as computed at the MP2/cc-pVTZ level) are also indicated. See ref 26 for a previous theoretical work on OCS·OCS. ^b Geometrical disposition corresponding to the reported experimental geometry (see ref 25). ^c MP4SDTQ//MP2 and QCISD(T)//MP2 single-point calculations.

The MP2/cc-pVTZ three-body contribution to the interaction energy for **MI** is -51 cm^{-1} . This stabilization is larger than for the $(\text{OCS})_2\cdot\text{CO}_2$ (-39 cm^{-1})¹¹ and $\text{OCS}\cdot(\text{CO}_2)_2$ (-12 cm^{-1})¹⁰ trimers.

A very important point to understand the process of cluster formation is the relation, if any, between the geometries of the three faces of the trimers and the possible geometries for the isolated dimer. Peebles and Kuczowski analyzed this aspect in terms of the changes in geometry experienced by the dimers upon addition of the third monomer to form the antiparallel (experimentally detected) vdW complex $(\text{OCS})_3$.⁶ We will carry out a similar analysis but this time based on the balance of the different contributions to the interaction energy as computed by the means of SAPT. The conclusions are then expected to be physically meaningful and will help us to throw some additional light on the nature of the interactions governing the formation of the trimer structure.

Table 5 collects the most stable structures for $(\text{OCS})_2$ according to ab initio calculations, and Table 6 shows the different contributions to the interaction energy in these dimer structures as well as in the dimer faces of the $(\text{OCS})_3$ vdW **MI** complex, as computed by SAPT.

The first interesting observation from Table 6 is that the induction contributions (E_{ind}) to the interaction energy are by no means negligible. As a matter of fact, such contributions are in most cases greater than the electrostatic contributions (E_{pol}) for the systems under study. That means that the use of semiempirical models with no inclusion of the induction forces should be considered with extreme caution. On the other hand, the most important stabilization contribution is that arising from the dispersion forces (E_{disp}), as expected for vdW complexes.²⁷

Peebles and Kuczowski reported that two of the dimer faces in the trimer (the parallel face and one of the antiparallel faces) are twisted from planarity by 32.7° (parallel face) and 23.8° (antiparallel face), respectively. The third face in $(\text{OCS})_3$ remains

basically planar (the S—C—C—S dihedral angle is 1.2°). Our calculations predict deviations from planarity of 21.5 , 29.4 , and 7.4° , respectively. On the other hand, Peebles and Kuczowski noted that the antiparallel face that is nearly planar has a much larger tilt away (S—C—C angles of 77.8 and 63.5° , respectively) from the isolated dimer structure (S—C—C angles of 78.2°) than the antiparallel face that has a large dihedral angle (S—C—C angles of 70.9 and 75.9° , respectively). The MP2/cc-pVTZ calculations predict the two monomers in the antiparallel faces not being too much tipped away from the parallel alignment (S—C—C angles of 76.3 and 76.1° for the antiparallel twisted face and 71.6 and 70.9° for the antiparallel nearly planar face).

Table 6 shows that the aforementioned geometrical departures of the faces of the trimer from the experimentally observed $(\text{OCS})_2$ vdW complex structure²⁵ have little effect on the corresponding nature of interactions. Indeed, the different contributions to the interaction energy for the antiparallel dimer faces [see OCS·OCS(A) and OCS·OCS(B) in Table 6] are quite similar to those computed for the $(\text{OCS})_2$ vdW complex structure OCS·OCS(a). In the case of OCS·OCS(A), both of the stabilizing (electrostatic, induction, and dispersion) and destabilizing (exchange) contributions are slightly greater in absolute value (about 50 cm^{-1}) than in the isolated dimer. For the OCS·OCS-(B) antiparallel face, all the contributions become smaller in absolute value than in the isolated dimer also by about 50 cm^{-1} . As a global effect, in the OCS·OCS(A) face the changes compensate each other, resulting an interaction energy close to that of the $(\text{OCS})_2$ isolated dimer OCS·OCS(a), while the OCS·OCS(B) face becomes somewhat less stable. Interestingly, this latter OCS·OCS(B) less stable face corresponds to the structure exhibiting deviations from planarity (the experimentally observed structure for the dimer is planar).²⁵

These observations are consistent with previous findings^{10,11} that the PESs for this type of vdW systems are rather flat. Indeed, such PESs are so flat that the experimental vibrationally averaged structure can be significantly different from the equilibrium structure. Appreciable changes in geometry have little energetic effects. Indeed, we carried out SAPT calculations on the two antiparallel faces using the experimental geometries,⁶ and we found quite similar interaction energies (-582 and -605 cm^{-1} , respectively).

We carried out an exhaustive SAPT analysis on the rest of barrel-like structures located on the PES, and we arrived at the same conclusion: the three dimer faces in each trimer are clearly related to some of the three possible dimer structures in Table 5. Thus, the structure **MI** is built up from dimers a, b, and c (see Table 5 for notation); **MII** from dimers b, b, and c; and **MIV** (see next) from dimers c, c, and c. Table 6 also contains SAPT information for structure **MIV** (see discussion to follow), and the corresponding information for structures **MII** and **MIII** is available as Supporting Information.

In the case of the planar dimers **MV** and **MVI**, the dimer faces do not resemble any isolated dimer structure with the exception of one of the faces in **MV** that is clearly related to dimer c (see Table 5). Consistently, these two planar structures are less stable than the barrel-like structures.

Why Is the Antiparallel Arrangement More Stable than the Parallel One? Comparison of SAPT data in Table 6 for **MI** and **MIV** structures makes clear why the antiparallel arrangement is the experimentally preferred structure. As mentioned previously, the three dimer faces in **MIV** correspond to slight variations (from an energy viewpoint) of the OCS·OCS-(c) parallel structure in Table 5, while for the **MI** complex, the three dimer faces are built up from a combination of two OCS·

TABLE 6: Contributions to the Interaction Energy of the Isolated Dimers and Dimer Faces in the Antiparallel Trimer MI and Parallel Trimer MIV as Computed by SAPT/aug-cc-pVDZ^a

	isolated dimers			MI		
	OCS·OCS(a) ^b	OCS·OCS(b) ^c	OCS·OCS(c) ^c	OCS·OCS(A)	OCS·OCS(B)	OCS·OCS(C)
$E_{\text{pol}}^{(10)}$	-742	-446	-584	-788	-606	-519
$E_{\text{pol,r}}^{(12)}$	34	96	37	46	-31	-5
$E_{\text{pol}}^{(1)}$	-708	-350	-547	-742	-637	-524
$E_{\text{ind,r}}^{(20)}$	-835	-282	-601	-893	-779	-604
$tE_{\text{ind}}^{(22)}$	24	-24	0	27	20	-2
$E_{\text{ind}}^{(2)}$	-811	-306	-601	-866	-759	-606
$E_{\text{disp}}^{(20)}$	-1420	-1007	-1257	-1452	-1390	-1286
$E_{\text{disp}}^{(2)}$	-1420	-1007	-1257	-1452	-1389	-1286
$E_{\text{exch}}^{(10)}$	1413	806	1168	1484	1364	1196
$E_{\text{exch}}^{(11)} + E_{\text{exch}}^{(12)}$	35	113	71	32	36	70
$E_{\text{exch}}^{(1)}$	1448	919	1239	1516	1400	1266
$E_{\text{exch-ind,r}}^{(20)}$	775	225	538	829	724	543
$tE_{\text{exch-ind}}^{(22)}$	-22	19	0	-25	-19	1
$E_{\text{exch-disp}}^{(20)}$	162	78	125	170	157	128
$E_{\text{exch}}^{(2)}$	915	322	663	974	862	672
$\delta E_{\text{int}}^{\text{HF}}$	-67	-49	-59	-71	-62	-61
$E_{\text{int}}^{\text{HF}}$	543	254	462	562	640	555
$E_{\text{int}}^{\text{CORR}}$	-1188	-725	-1024	-1203	-1227	-1094
$E_{\text{int}}(\text{SAPT})$	-645	-472	-561	-641	-586	-538
E_{RELAX}^d	0	2	1	1	1	1
$E_{\text{int}}^{\text{SUP}}(\text{NCP})^e$	-888	-700	-789	-880	-821	-765
$E_{\text{int}}^{\text{SUP}}(\text{CPR})^e$	-559	-421	-490	-549	-506	-463

	MIV		
	OCS·OCS(A)	OCS·OCS(B)	OCS·OCS(C)
$E_{\text{pol}}^{(10)}$	-498	-589	-521
$E_{\text{pol,r}}^{(12)}$	-9	34	0
$E_{\text{pol}}^{(1)}$	-507	-555	-521
$E_{\text{ind,r}}^{(20)}$	-573	-611	-586
$tE_{\text{ind}}^{(22)}$	-4	-3	-3
$E_{\text{ind}}^{(2)}$	-574	-614	-589
$E_{\text{disp}}^{(20)}$	-1267	-1261	-1276
$E_{\text{disp}}^{(2)}$	-1267	-1261	-1276
$E_{\text{exch}}^{(10)}$	1162	1194	1179
$E_{\text{exch}}^{(11)} + E_{\text{exch}}^{(12)}$	74	73	75
$E_{\text{exch}}^{(1)}$	1236	1267	1254
$E_{\text{exch-ind,r}}^{(20)}$	513	549	524
$tE_{\text{exch-ind}}^{(22)}$	4	2	3
$E_{\text{exch-disp}}^{(20)}$	124	128	125
$E_{\text{exch}}^{(2)}$	641	679	652
$\delta E_{\text{int}}^{\text{HF}}$	-58	-58	-59
$E_{\text{int}}^{\text{HF}}$	546	485	537
$E_{\text{int}}^{\text{CORR}}$	-1079	-1027	-1077
$E_{\text{int}}(\text{SAPT})$	-533	-542	-539
E_{RELAX}^c	8	4	3
$E_{\text{int}}^{\text{SUP}}(\text{NCP})^d$	-768	-613	-627
$E_{\text{int}}^{\text{SUP}}(\text{CPR})^d$	-474	-336	-341

^a All numbers in cm⁻¹. NCP and CPR mean uncorrected and CP-corrected (including fragment relaxation energies) interaction energies, respectively.

^b Experimentally reported structure (see structure a in Table 5 and ref 25). ^c Unobserved structures located by ab initio exploration of the potential energy surface (see structures b and c in Table 5). ^d Relaxation energy. ^e MP2/aug-cc-pVDZ interaction energies.

OCS(a) (antiparallel) + OCS·OCS(c) (parallel) structures. As OCS·OCS(a) is 56 cm⁻¹ more stable than OCS·OCS(c) at the MP2/cc-pVTZ level of theory (see Table 5), the above arguments lead to 112 cm⁻¹ in favor of the antiparallel arrangement that agrees rather well with the 109 cm⁻¹ energy difference

between **MI** and **MIV** (see Table 3; the MP2/cc-pVTZ three-body corrections for **MI** and **MIV** are very similar: 51 and 47 cm⁻¹, respectively).

Another interesting fact emerging from the data collected in Table 6 is that SAPT (BSSE-free) interaction energies lie

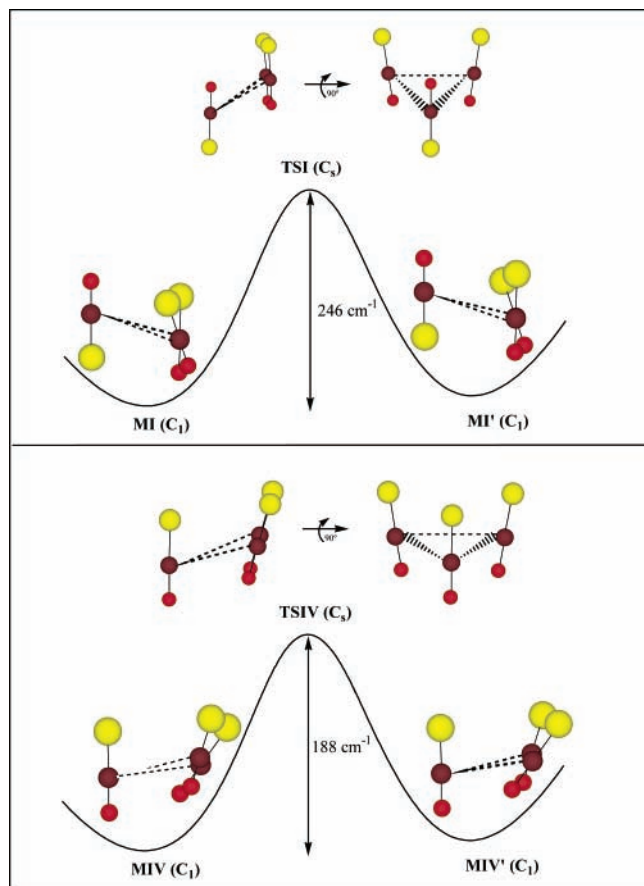


Figure 2. Transition structures connecting two enantiomeric forms of **MI** (**TSI**) and **MIV** (**TSIV**) structures. Energy barriers (including zero-point energy) were estimated at the QCISD(T)/aug-cc-pVDZ//MP2/aug-cc-pVDZ level of theory.

between the supermolecular uncorrected and the corrected corresponding values. This systematic behavior, already observed in previous studies on similar systems,^{10,11} can be interpreted in terms of the overcorrection commonly associated with the use of Boys–Bernardi's CP method to correct for BSSE.²⁸

Dynamics. According to Connelly et al.,⁴ the microwave spectra of the (OCS)₃ vdW complex shows a fine doubling of less than 20 kHz for many lines corresponding to a- and c-type transitions that is associated with the interconversion between two enantiomeric forms of structures **MI** and **MIV** (see Figure 2). After the work of Peebles and Kuczkowski,⁶ it is clear that **MI** is the experimentally detected structure. The ab initio calculations presented in this work agree with that observation, predicting **MI** to be lower in energy than **MIV**. Therefore, the interconversion giving rise to the splittings must be that corresponding to the structure **MI**.

Figure 2 shows the transition structures representing the interconversions between two enantiomeric forms of **MI** (**TSI**) and **MIV** (**TSIV**), respectively, as located on the MP2/cc-pVTZ PES of (OCS)₃. The computed barriers are about twice the ones estimated by Connelly et al. using Muentner's semiempirical potential⁵ and with no geometrical optimization of the proposed transition structures.⁴ The relatively high ab initio energy barrier associated with **TSI** is consistent with the rather small splittings reported by Connelly et al. (about 20 kHz)⁴ and with the fact that no splittings were observed when the ¹⁸OCS and O¹³CS isotopic species were employed.⁶ Bearing in mind that the barrier associated with the tunneling motion is by no means negligible, as the signals become less intense because of isotopic substitu-

tions, the observation of the line splitting is expected to deteriorate. The zero-point energy contributions for **MI** and **TSI** are practically the same as a consequence of the fact that both structures exhibit a rather similar geometry, so they do not make appreciable contributions to the energy barrier. A quantitative determination of the magnitude of the microwave line splitting associated with the tunneling motion is out of the scope of the present work.

Conclusions

Ab initio calculations were carried out to explore the potential energy surface of the (OCS)₃ vdW complex. Six minima structures were located and characterized. Among them, one exhibiting an antiparallel arrangement is the most stable structure. Its geometry, as estimated at the MP2/cc-pVTZ level, agrees reasonably well with that predicted from pulsed nozzle Fourier transform microwave spectroscopy. A second structure with a parallel arrangement resulted in being slightly less stable.

The application of the Symmetry Adapted Perturbation Theory led to a number of interesting conclusions: (a) dispersion forces are the dominant component of the interaction energy. (b) The induction component is by no means negligible. Therefore, the application of semiempirical models with no consideration of induction forces seems not to be appropriate. (c) The three dimer faces in each trimer structure are slight variations of the possible structures (not all of them observed experimentally) of the isolated (OCS)₂. (d) The previous point, together with the fact that the unobserved parallel (OCS)₂ is less stable than the experimentally detected antiparallel (OCS)₂, allow one to rationalize the experimental fact that only the antiparallel (OCS)₃ vdW complex has been observed.

Finally, two transition structures representing the interconversion of enantiomeric forms corresponding to both the parallel and the antiparallel (OCS)₃ vdW complexes were located on the MP2/cc-pVTZ potential energy surface. The relative high energy barriers associated with them are consistent with the very small splittings observed in the rotational spectra of the normal species that disappear when the ¹⁸OCS and O¹³CS isotopic forms are employed.

Acknowledgment. Partial financial support by DGES (Madrid, Spain) under Project BQU2001-3660-C02-01 is greatly acknowledged.

Supporting Information Available: Figures and tables of geometrical parameters. This material is available free of charge via the Internet at <http://pubs.acs.org>.

References and Notes

- Castleman, A. W., Jr.; Brown, K. H., Jr. *J. Phys. Chem.* **1996**, *100*, 12911.
- Legon, A. C. in *Atomic Molecular Beam Methods*; Scoles, G., Ed.; Oxford University Press: Oxford, 1992; Vol. 2, Ch. 9.
- Leopold, K. R.; Fraser, G. T.; Novick, S. E.; Klemperer, W. *Chem. Rev.* **1994**, *94*, 1807.
- Connelly, J. P.; Bauder, A.; Chisholm, A.; Howard, B. J. *Mol. Phys.* **1996**, *88*, 915.
- Muentner, J. S. *J. Chem. Phys.* **1991**, *94*, 2781.
- Peebles, R. A.; Kuczkowski, R. L. *J. Phys. Chem. A* **1999**, *103*, 6344.
- Stone, A. J. *The Theory of Intermolecular Forces*; Clarendon Press: Oxford, 1996.
- Peebles, R. A.; Kuczkowski, R. L. *J. Chem. Phys.* **2000**, *112*, 8839.
- Peebles, S. A.; Kuczkowski, R. L. *J. Mol. Struct. (THEOCHEM)* **2000**, *500*, 391.
- Valdés, H.; Sordo, J. A. *J. Comput. Chem.* **2002**, *23*, 444.
- Valdés, H.; Sordo, J. A. *J. Phys. Chem. A* **2002**, *106*, 3690.
- Valdés, H.; Sordo, J. A. *J. Phys. Chem. A* **2003**, *107*, 899.

- (13) Bukowski, R.; Jankowski, P.; Jeziorski, B.; Jeziorski, M.; Kucharski, S. A.; Moszynski, R.; Rybak, S.; Szalewicz, K.; Willians, H. L.; Wormer, P. E. S. *SAPT96: An ab initio Program for Many-Body Symmetry-Adapted Perturbation Theory Calculations of Intermolecular Interaction Energies*; University of Delaware and University of Warsaw, 1996.
- (14) Rayón, V. M.; Sordo, J. A. *J. Chem. Phys.* **1997**, *107*, 7912.
- (15) Rayón, V. M.; Sordo, J. A. *J. Chem. Phys.* **1999**, *110*, 377.
- (16) Rayón, V. M.; Sordo, J. A. *Chem. Phys. Lett.* **2001**, *341*, 575.
- (17) Hehre, W. J.; Radom, L.; Schleyer, P. v. R.; Pople, J. A. *Ab initio Molecular Orbital Theory*; Wiley: New York, 1986.
- (18) Dunning, T. H., Jr. *J. Chem. Phys.* **1989**, *90*, 1007.
- (19) Kendall, R. A.; Dunning, T. H., Jr. *J. Chem. Phys.* **1992**, *96*, 6796.
- (20) Bader, R. F. W. *Atoms in Molecules. A Quantum Theory*; Oxford University Press: New York, 1990.
- (21) Boys, S. F.; Bernardi, F. *Mol. Phys.* **1970**, *19*, 553.
- (22) Sordo, J. A. *J. Chem. Phys.* **2001**, *114*, 1974.
- (23) Frisch, M. J.; Trucks, G. W.; Schlegel, H. B.; Scuseria, G. E.; Robb, M. A.; Cheeseman, J. R.; Zakrzewski, V. G.; Montgomery, J. A., Jr.; Stratmann, R. E.; Burant, J. C.; Dapprich, S.; Millam, J. M.; Daniels, A. D.; Kudin, K. N.; Strain, M. C.; Farkas, O.; Tomasi, J.; Barone, V.; Cossi, M.; Cammi, R.; Mennucci, B.; Pomelli, C.; Adamo, C.; Clifford, S.; Ochterski, J.; Petersson, G. A.; Ayala, P. Y.; Cui, Q.; Morokuma, K.; Malick, D. K.; Rabuck, A. D.; Raghavachari, K.; Foresman, J. B.; Cioslowski, J.; Ortiz, J. V.; Stefanov, B. B.; Liu, G.; Liashenko, A.; Piskorz, P.; Komaromi, I.; Gomperts, R.; Martin, R. L.; Fox, D. J.; Keith, T.; Al-Laham, M. A.; Peng, C. Y.; Nanayakkara, A.; Gonzalez, C.; Challacombe, M.; Gill, P. M. W.; Johnson, B. G.; Chen, W.; Wong, M. W.; Andres, J. L.; Head-Gordon, M.; Replogle, E. S.; Pople, J. A. *Gaussian 98*; Gaussian, Inc.: Pittsburgh, PA, 1998.
- (24) Chalasinski, G.; Szczesniak, M. M. *Mol. Phys.* **1988**, *63*, 205.
- (25) Randall, R. W.; Wilkie, J. M.; Howard, B. J.; Muentzer, J. S. *Mol. Phys.* **1990**, *69*, 839.
- (26) Bone, R. G. A. *Chem. Phys. Lett.* **1993**, *206*, 260.
- (27) Hobza, P.; Zahradnik, R. *Intermolecular Complexes. The Role of van der Waals Systems in Physical Chemistry and in Biodiscipline*; Academia: Prague, 1988.
- (28) López, J. C.; Alonso, J. L.; Alonso, F. J.; Rayón, V. M.; Sordo, J. A. *J. Chem. Phys.* **1999**, *111*, 6363 and references therein.